9-1-2016

COX-2 Induces Breast Cancer Stem Cells via EP4/PI3K/AKT/NOTCH/WNT Axis

Mousumi Majumder

Xiping Xin

Ling Liu

Elena Tutunea-Fatan
Physiology and Pharmacology

Mauricio Rodriguez-Torres

See next page for additional authors

STEM CELLS®

CANCER STEM CELLS

COX-2 Induces Breast Cancer Stem Cells via EP4/PI3K/AKT/NOTCH/WNT Axis

MOUSUMI MAJUMDER,[a] XIPING XIN,[a] LING LIU,[a] ELENA TUTUNEA-FATAN,[b] MAURICIO RODRIGUEZ-TORRES,[a] KRISTA VINCENT,[a,c] LYNNE-MARIE POSTOVIT,[a,c] DAVID HESS,[b,d] PEEYUSH K. LALA[a,e]

Key Words. Breast cancer • Cyclo-oxygenase-2 • EP4 • Stem-like cell • NOTCH/WNT

[a]Department of Anatomy and Cell Biology, [b]Physiology and Pharmacology, [e]Oncology, Schulich School of Medicine and Dentistry, University of Western Ontario, London, Ontario, Canada; [c]Department of Oncology, University of Alberta, Edmonton, Alberta, Canada; [d]Krembil Centre for Stem Cell Biology, Robarts Research Institute, London, Ontario, Canada

Correspondence: Dr. Peeyush K. Lala, MD, Ph.D., DSc., Department of Anatomy and Cell Biology, Schulich School of Medicine and Dentistry, University of Western Ontario, 1151 Richmond St., London, Ontario N6A 5C1, Canada. Fax: 519-661-3936; e-mail: pklala@uwo.ca

Received September 21, 2015; accepted for publication April 18, 2016; first published online in STEM CELLS *EXPRESS* June 14, 2016.

1066-5099/2016/$30.00/0

http://dx.doi.org/10.1002/stem.2426

ABSTRACT

Cancer stem-like cells (SLC) resist conventional therapies, necessitating searches for SLC-specific targets. We established that cyclo-oxygenase(COX)-2 expression promotes human breast cancer progression by activation of the prostaglandin(PG)E-2 receptor EP4. Present study revealed that COX-2 induces SLCs by EP4-mediated NOTCH/WNT signaling. Ectopic COX-2 over-expression in MCF-7 and SKBR-3 cell lines resulted in: increased migration/invasion/proliferation, epithelial-mesenchymal transition (EMT), elevated SLCs (spheroid formation), increased ALDH activity and colocalization of COX-2 and SLC markers (ALDH1A, CD44, β-Catenin, NANOG, OCT3/4, SOX-2) in spheroids. These changes were reversed with COX-2-inhibitor or EP4-antagonist (EP4A), indicating dependence on COX-2/EP4 activities. COX-2 over-expression or EP4-agonist treatments of COX-2-low cells caused up-regulation of *NOTCH/WNT* genes, blocked with PI3K/AKT inhibitors. NOTCH/WNT inhibitors also blocked COX-2/EP4 induced SLC induction. Microarray analysis showed up-regulation of numerous SLC-regulatory and EMT-associated genes. MCF-7-COX-2 cells showed increased mammary tumorigenicity and spontaneous multiorgan metastases in NOD/SCID/IL-2Rγ-null mice for successive generations with limiting cell inocula. These tumors showed up-regulation of VEGF-A/C/D, Vimentin and phospho-AKT, down-regulation of E-Cadherin and enrichment of SLC marker positive and spheroid forming cells. MCF-7-COX-2 cells also showed increased lung colonization in NOD/SCID/GUSB-null mice, an effect reversed with EP4-knockdown or EP4A treatment of the MCF-7-COX-2 cells. *COX-2/EP4/ALDH1A* mRNA expression in human breast cancer tissues were highly correlated with one other, more marked in progressive stage of disease. In situ immunostaining of human breast tumor tissues revealed co-localization of SLC markers with COX-2, supporting COX-2 inducing SLCs. High *COX-2/EP4* mRNA expression was linked with reduced survival. Thus, EP4 represents a novel SLC-ablative target in human breast cancer. STEM CELLS *2016;34:2290–2305*

SIGNIFICANCE STATEMENT

This study presents novel mechanistic findings that cyclo-oxygenase (COX)-2 induces stem-like cells (SLC) in human breast cancer by activation of the prostaglandin E-2 receptor EP4 leading to up-regulation of NOTCH/WNT via PI3K/AKT signaling pathways. COX-2 induced SLC properties resulting from EP4/PI3K/AKT activation were confirmed with mammary site transplants and lung colonization of COX-2 over-expressing cells in immune deficient mice, showing multi-organ metastasis. In human breast cancer tissues, (a) SLC markers were localized mostly to COX-2+ cells; (b) *COX-2/EP4/ALDH1A* mRNAs were highly correlated with one another; and (c) high *COX-2/EP4* expression were associated with reduced survival. We suggest that EP4 antagonist, which spare cardio-protective prostanoids, are better suited than COX-2 inhibitors for SLC-reduction in this disease.

INTRODUCTION

Breast cancer strikes one in eight women in North America and accounts for the second highest cause of cancer-related mortality in females, mostly ascribable to metastatic disease [1]. Traditional treatment modalities complemented by target-oriented therapies including HER-2-blockade have recently prolonged the survival. However, many patients still remain unresponsive or develop resistance to the target-oriented drugs, indicating the need for personalized therapeutics [2].

A tumor cell subpopulation known as "stem-like cells" (SLC)s is thought to play a major role in tumor progression, metastasis,

and recurrence after traditional therapy [3]. In support, several studies have shown a positive association of embryonic stem (ES) cell markers such as OCT4, NANOG, and SOX-2 with cancer metastasis [4, 5]. Whether arising from mutations in tissue-specific stem/progenitor cells or from dedifferentiation of breast cancer cells, SLCs are characterized by the expression of certain markers. Breast cancer-associated SLCs have been reported as CD44 high, CD24 low and ALDH positive [6]. In addition, proteins such as Snail, ZEB1, and Twist, involved in epithelial-mesenchymal transition (EMT), have also been linked with SLC phenotype [7–9].

Cyclo-oxygenase (COX)-2, an inflammation-associated enzyme, plays a key role in tumor initiation in tissues subjected to chronic inflammation [10, 11]. COX-2 over-expression is both a signature as well as a driver of tumor progression and metastasis in a variety of epithelial cancers including breast, and COX-2 inhibitors have shown chemo-preventive and therapeutic effects [12]. COX-2 expression, found in 40%-50% of primary human breast cancers, is a marker for increased morbidity and poor survival [13]. Our studies in murine and human breast cancer models established that elevated COX-2 expression by breast cancer cells promotes tumor progression via multiple mechanisms: inactivation of host anti-tumor immune cells [14], enhancement of cancer cell migration and invasiveness [15, 16], promotion of tumor-associated angiogenesis [15], and lymphangiogenesis resulting from up-regulation VEGF-C/-D [5, 17, 18], induction of SLC and elevation of an oncogenic microRNA-526b [19].

PGE2, the major product of the COX-2 activation cascade can bind to four G protein coupled receptors (EP1-EP4) having distinct signaling capabilities [20]. Most of the above-mentioned COX-2 mediated events promoting breast cancer progression was due to activation of the PGE2 receptor EP4 on tumor and host cells by endogenous PGE2 [5, 17, 18]. While Gs coupled EP2 and EP4 receptors share signaling via the cAMP/PKA pathway, EP4 also signals through the phosphatidylinositol 3-kinase (PI3K)/AKT pathway [21, 22]. This differential signaling mechanism utilized by the EP4 receptor protects cells from apoptosis, making EP4 antagonists (EP4A) attractive alternatives to COX-2 inhibitors. Furthermore, thrombo-embolic side effects of COX-2 inhibitors [23, 24] can be avoided with EP4A since they do not inhibit cardio-protective prostanoids such as PGI2 [25]. We validated this contention in a syngeneic mouse breast cancer model, in which an EP4A at nontoxic doses were as effective as COX-2 inhibitors in exerting antitumor, antimetastatic, and SLC-ablative effects [5]. In the present study, we test the roles of EP4 and its putative signaling pathways in SLC induction in human breast cancer.

NOTCH and WNT signaling pathways, active during embryonic development, are also aberrantly activated during tumor progression. Both NOTCH [26, 27] and WNT [28, 29] pathways promote metastatic phenotypes in breast cancer cells. WNT/β-catenin inhibition was shown to be SLC-reductive in breast cancer [30]. PGE2, the major bioactive product of the COX-2 cascade, can activate components of the WNT signaling system [31]. However, COX-2/EP4 stimulation of WNT and NOTCH signaling pathways in breast cancer has not been documented.

While HER-2 is a major determinant of breast cancer progression, in murine models many HER-2 actions were COX-2 mediated [32, 33]. We established that lymphangiogenic functions of HER-2 in human breast cancer are also COX-2 dependent [34]. In the present study, we asked whether COX-2 or EP4 activation stimulates SLCs in both HER-2- and HER-2+ breast cancer cells by up-regulating NOTCH and WNT. We herein demonstrate that COX-2 increases breast cancer SLCs via EP4/PI3K-dependent induction of NOTCH/WNT signaling. In human breast cancer tissues, we found that SLC markers were localized mostly to COX-2+ cells and COX-2/EP4/SLC mRNAs were highly correlated with one another. Finally, high COX-2/EP4 mRNAs were associated with reduced survival. These studies establish the roles of COX-2/EP4 in SLC induction via PI3K/AKT/WNT/NOTCH pathways and further endorse EP4 as a therapeutic target in human breast cancer.

Materials and Methods

Ethics Statements

The human breast cancer and the adjacent noncancerous tissues used in this study were obtained from the Ontario Institute for Cancer Research (OICR) repository (Ontario Tumor Bank, Toronto, CA) based on approval by their Ethics Board. Use of mice was approved by the Animal Use Subcommittee of this University of Western Ontario, according to the guidelines of the Canadian Council on Animal Care.

Cell Lines and Culture Conditions

Human breast cancer cell lines (MCF-7, SKBR-3, MDA-MB-468, MDA-MB-231, Hs578T, and T47D) were purchased from American Type Culture Collection (ATCC, Rockville, MD, USA) and maintained according to ATCC protocol. MCF10A (COX-2, ER, HER-2-) mammary epithelial cell line is a kind gift of Dr. Moshmi Bhattacharya, University of Western Ontario. MCF-7 (COX-2-low, ER+, HER2−, nonmetastatic) and SKBR-3 (COX2−, ER−, HER2+, weakly metastatic) cells were transfected with 2 μg of either pCMV-IRES2-EGFP-vector (Mock) or pCMV-IRES2-EGFP-COX-2 expression plasmids (kind gift of Dr. Michael Archer, University of Toronto) using the Amaxa Cell Line Nucleofector Kit V (Lonza, Walkersville, MD) and the P-020 or E-009 program for MCF-7 cells or SKBR-3 cells respectively, according to the manufacturer's protocol. MCF-7-COX-2 and SKBR3-COX-2 and their respective mock cell lines were maintained in regular media with Geneticin® (GIBCO, ON, CA) at 500 μg/ml. We knocked-down EP4 (using same protocol) in MCF-7-COX-2 cells using shRNA plasmids (cat#sc-40173-SH) from Santa Cruz, Dallas, TX and stable cell lines named MCF-7-COX-2-Mock and MCF-7-COX-2-EP4KD, were maintained in regular media with Puromycin selection (300 ng/ml).

Drugs and Reagents

All in vitro concentrations of drugs were chosen as reported earlier [5, 19]. NS-398 (COX-2 inhibitor, 20 μM), 10 μM each of PGE2 (nonselective EP ligand) and PGE1OH (EP4 agonist) were purchased from Cayman Chemical (Ann Arbor, MI). ONO-AE3-208 (selective EP4 antagonist, 5 μM) was a gift of ONO Pharmaceuticals, Osaka, Japan. PI3K inhibitors (10 μM each) Wortmannin (WM) and LY-204002 (LY) were purchased from Sigma-Aldreich (St. Louis, MO). DMSO (solvent) served as control. We used WNT inhibitor rhDkk-1 (5 and 10 μM) from R&D Systems, Minneapolis, MN and NOTCH inhibitor

DAPT (50 and 100 ng) from Sigma-Aldreich, 0.3% BSA in PBS and DMSO served as vehicle control, respectively.

Real-Time PCR

We used RNeasy Kit (Qiagen, ON, CA) for RNA extraction and cDNA was synthesized with High Capacity Reverse Transcription Kit (Applied Biosystems, Foster City, CA). To quantify COX-2 (*PTGS2*), EP4 (*PTGER4*), E-Cadherin (*CDH1*), Vimentin (*VIM*), *TWIST1*, *SNAI1*, *ZEB1*, N-Cadherin (*CDH2*), *NOTCH (1-3)*, *HES1, HES6, AXIN1, AXIN2, c-MYC*, *Cyc-D1* (*CCND1*) and β-actin (*ACTB*) genes, we used human quantitative TaqMan Gene Expression probes from Applied Biosystems. Negative ΔCt values reflect higher mRNA expression in tissue samples. We also conducted semi-quantitative RT-PCR as described previously [17] for *VEGF-A/C/D, EPs* and *GAPDH*, a primer list given in Supporting Information Table 1.

Protein Detection and Measurement with Western Blots

Protein (15-20 μg) was separated on 10% SDS-PAGE gel to immuno-blot and quantify VEGF-A (sc-507), VEGF-C (sc-1881), VEGF-D (sc-13085), COX-2 (sc-1747), using antibodies (1:500 dilutions) from Santa Cruz Biotechnology, Dallas, TX. Monoclonal GAPDH antibody (MAB374) was from Millipore, Billerica, MA. Antibodies to ERK1/2 and phospho-ERK1/2 (9102 and 9101S), AKT, phospho-AKT-Ser473 (9272, 9271), E-Cadherin (3195), Vimentin (5741) (used at 1: 1:500 to 1:1,000 dilutions) were purchased from Cell Signaling, Danvers, MA. IRDye-800 conjugated antirabbit IgG, antigoat IgG and Alexa 680 conjugated antimouse IgG were used as secondary antibodies, as appropriate (LI-COR, Lincoln, NE).

Migration, Invasion, and Proliferation Assays

For migration assays, 6×10^4 cells in 300 μl basal media were added to the upper chamber of transwells including a multiporous polycarbonate membrane (8 μm pore size) insert Tewksbury, and placed in a 24-well plate (Corning Costar Corporation, Cambridge, MA). For invasion assays, cell inserts were coated with Matrigel (1:100 in basal media; BD Biosciences, Mississauga, ON, CA). The lower chamber contained 700 μl of either serum-free media or 2% FBS-supplemented media. Cells completing migration at 24 hours or invasion at 48 hours at 37°C were quantified as reported earlier [15, 16, 35]. BrdU ELISA (Roche Applied Science, Indianapolis, IN) was used to measure proliferation of MCF-7 and MCF-7-derived cell lines at 6 hours, and SKBR-3 and SKBR-3-derived cell lines at 8 hours [35].

Spheroid Formation

Cells were plated on ultra-low attachment plates (Corning Costar Corporation, Cambridge, MA) at dilution of 1 cell/100 μl or 2×10^4 cells/2ml, as previously described [5, 19, 36]. Spheroids were harvested and their RNA extracted to conduct real-time qPCR for target gene expression. Images of spheroid were captured under a light microscope and the number and perimeter of spheroids calculated using ImageJ (National Institutes of Health, Bethesda, MD).

Detection of SLC Having ES Cell Associated Markers

Spheroids were subjected to dual immuno-staining for COX-2 (Abcam, Cambridge, MA) and ALDH1A, CD44, OCT-3/4, SOX-2, NANOG, β-Catenin, with antibodies (1:300 dilution) from BD biosciences, and staining conducted as reported previously [5].

Fluorescence-Activated Cell Sorting

Breast cancer SLCs have been reported to be ALDH-high/CD44 + CD24− [2, 37]. We used ALDEFLUOR assay kit (StemCell Technologies, BC, Canada), followed by staining for CD44-PE-Cy7 (560533) and CD24-PE (560991) conjugated antibodies (BD Biosciences, San Jose, CA). Cells were concurrently labeled with 7-aminoactinomycin (7-AAD, #560253) to test viability and fluorescently conjugated IgG isotype was applied as negative controls (BD Biosciences). While staining for ALDH activity alone, we used top 20% as $ALDH^{high}$ and bottom 20% as $ALDH^{low}$ [37]. To identify the CD44 + CD24− subset, sorting for $ALDH^{high}$ was set at top 10%, and $ALDH^{low}$ at bottom 10%. All markers were examined in monolayer and spheroid dissociated cells. Cell purity for each sorted population was 98%-99%.

Microarray

We conducted gene microarrays (quadruplicate measurements) comparing mRNA expression changes between MCF-7-COX-2 and Mock-transfected control cells, using Affymetrix Genechip Micro-Array 1.0 as per manufacturer's protocol. ANOVA with a nominal alpha value set to 0.05 was used to identify significant changes, followed by Benjamini-Hochberg multiple testing correction in order to reduce the false positive rate. Results (fold change ±1.5) were then separated into significant increases or decreases ($p < .05$), and used in a cross platform analysis. Some results were verified with RT-PCR described later.

Experimental Metastasis Assay in GUSB Null/NOD/SCID/MPSVII Mice

We used beta-glucuronidase (GUSB)-deficient NOD/SCID/mucopolysaccharidosis type VII mice to identify transplanted human tumor cells at single cell resolution [38] by virtue of their constitutive GUSB activity. Following tail vein injection of 5×10^5 cells of MCF-7-Mock, MCF-7-COX-2, MCF-7-COX-2-Mock, and MCF-7-COX-2-EP4KD cells in 350 μl PBS, mice were sacrificed at 4 weeks (to assess micrometastases) and 6 weeks (to assess macro-metastases). Each cell inoculum used eight mice. In another set of mice, we injected MCF-7-COX-2 cells pretreated with EP4A (5 μM) for 7 days before injection, 0.3% DMSO in PBS served as vehicle treatment. Excised lungs, brain, liver, spleen, and kidneys were cut into two halves, one half frozen in OCT (Sakura Finetek, Torrance, CA) to assess GUSB by histological analysis. Serial 10 μm-thick frozen sections were fixed in 10% buffered formalin, blocked with mouse-on-mouse reagent (Vector Laboratories, Burlingame, CA) and analyzed for GUSB-stained human cells [38]. At least 10 sections were acquired from evenly spaced areas, and the average number of metastases per organ was calculated. Other halves of all organs were stained with H&E [5, 18].

To measure cell proliferation in vivo we used Click-iT® EdU Alexa Fluor® 488 Imaging Kit (Invitrogen, Molecular Probes, Carlsbad, CA). EdU was injected intravenously 12 hours before sacrifice in these mice following manufacturer protocol.

Tumor Growth and Spontaneous Metastasis in NOD/SCID/IL2Rγ Null Mice

These T, B, and NK cell deficient mice are excellent hosts for tumor xenografts [39]. In the first experiment (**named F1**), mice ($n = 4$ for each cell line) were randomized as follows: subcutaneous inocula of either MCF-7-Mock or MCF-7-COX-2 (5×10^5 or 5×10^4) cells suspended in growth factor-reduced Matrigel (3.5 mg in 0.5 ml EMEM) were implanted in both inguinal and axillary mammary regions (i.e., four sites per mouse) close to the nipples. Thus, the *n* value of tumors for each group was 16. Individual mice received the same tumor line and inoculums dose. Matrigel implants alone served as the negative control in five additional mice [40].

Tumor volumes were measured as $0.5 \times a^2b$, from the minimum (a) and maximum (b) diameters at 2-day intervals, as reported previously [5, 18, 35] until sacrifice on day 73. Upon retrieval, the implants were photographed and sliced into three pieces, for RNA and protein extraction and retransplantation. Excised lungs, livers, spleens, kidneys, and brains were cut into two pieces, one frozen for immunohistochemical analysis of HLA and another fixed for H&E staining. Lungs were harvested after inflation with PBS. At least three semiserial 10 μm thick sections of these organs from each animal were stained with mouse antihuman HLA antibody (1:100 dilution, Sigma-Aldrich) to detect tumor cells [19].

Serial Transplantation of F1 Tumors into Another Set of Mice (F2)

We named second-generation tumors as **F2**. Excised F1 tumors were cut into small pieces, one piece subjected to histology. Other pieces were minced and processed in a 50 ml conical flask with 10-15 ml of tumor-collagenase solution (Millipore) on a shaker bath (37°C) for 2-3 hours to digest larger fragments. Then 10 ml HBSS/2% FBS (Thermo Fisher Scientific, Waltham, MA) was added and cells sieved through a 40 μm filter, spun down at 1,000 rpm for 5 minutes. The cell pellets were washed thrice in an identical manner and resuspended in 3 ml 0.25% Trypsin for 5 minutes at 37°C and neutralized with 5 ml DMEMF12/10%FBS. Ten-milliliter HBSS was then added and cells passed sequentially through a 100 μm filter and 40 μm Nylon Cell Strainer. The elutes were spun at 1,000 rpm for 5 minutes and cell pellets suspended with DMEM-F12 (Thermo Fisher Scientific, Waltham, MA) in diluted Matrigel as described earlier [18] at two different inocula (5×10^4 and 5×10^3 cells). The rest of the protocol was the same as in F1. Remaining cells were cultured in DMEMF12/10% FBS with 500 μg/ml Geneticin for further assays.

Human Tissue Samples

mRNA Expression. To examine the clinical relevance of *COX-2, EP2, EP4, ALDH1A* mRNA expression in breast cancer, we obtained frozen female human breast tumor ($n = 105$) and control ($n = 20$) tissues (adjacent nontumor tissues verified as tumor-free) from the Ontario Tumor Bank. Demographic, tobacco/alcohol habits, ER, PR, and HER-2 status of tumor and control of tissue donors are summarized in Supporting Information Table 2. The majority of the patients (>80%, data not provided) had a history of some unspecified cancer in the family. Of the tumor tissues, 76% were ER positive, 62.9% PR positive, 20% HER2 positive, and 9.5% triple (ER/PR/HER2) negative. Tumor samples were classified in five stages (0-IV) with respect to TNM following Canadian Cancer Society staging.

In Situ Detection of SLC Markers. We conducted immunostaining for COX-2, NANOG, SOX2, ALDH, and CD44 in deparaffinised and rehydrated tissue sections as follows. Sections were sequentially treated with xylene (5 minutes, 3X) followed by graded ethanol (100%, 90%, 70%, 2 minutes each, 2X) and washed with tap water followed by PBS (5 minutes, 3X). Background was blocked with Sniper (Biocare Medical, Concord, CA, 10 minutes) and washing with PBS. Sections were then incubated with primary antibodies (1:100 dilutions) for 1h at room temperature and washed with PBS (5 minutes, 3X). Then they were treated with appropriate secondary antibodies (1:500 dilutions) for 45 minutes, followed by washing with PBS (5 minutes, 3X). Finally, cell nuclei were stained with DAPI (10 minutes), followed by washes with PBS (5 minutes, 3X).

Survival Analyses

Coded patient survival data were extracted from the Cancer Genome Atlas (TCGA) clinical information [41]. Patient survival was calculated as time in months elapsed from the date of diagnosis until the date of last contact. Kaplan-Meier curves for overall survival associated with COX-2 and EP4 expression were conducted in 942 primary breast carcinomas. A cutoff *p* value ($p < .05$) was determined using log-rank test.

Statistical Analysis

Statistical calculations were performed using GraphPad Prism software version 5 (La Jolla, CA). All parametric data were analyzed with one-way ANOVA followed by Tukey-Kramer or Dunnett post-hoc comparisons. Student's *t* test was used for comparing two data sets and Pearson's coefficient to assess statistical correlations. Significant differences between means were accepted at $p < .05$.

Results

In Vitro Studies

Stable COX-2 Over-Expression Induces Breast Cancer SLCs via EP4-Dependent Pathway. COX-2 has been shown to induce aggressive phenotypes in multiple cancer types [10–12]. In order to determine the effects of ectopic COX-2 on breast cancer cell phenotype, we over-expressed COX-2 in MCF-7 and SKBR-3 cell lines. Following selection these cells expressed COX-2 mRNA and protein levels similar to MDA-MB-231 cells (Supporting Information Fig 1A, 1B). As expected from our previous work with endogenous COX-2 [16-19] ectopically expressed COX-2 in MCF-7-COX-2 and SKBR-3-COX-2 cells increased migration (Fig. 1A), invasion (Fig. 1B) and proliferation (Fig. 1C) of both MCF-7-COX-2 and SKBR-3-COX-2 cells. Furthermore, MCF-7-COX-2 cells displayed down-regulation of estrogen receptor (Supporting Information Fig. 1C) and up-regulation of VEGF-A/C/D and all EP receptors (Supporting Information Fig. 1D). Additionally, the COX-2 inhibitor NS398 and EP4 antagonist ONO-AE3-208 significantly inhibited migration, invasion, and proliferation in COX-2 over-expressing cells. (Fig. 1A-1C). The same dosages of drugs did

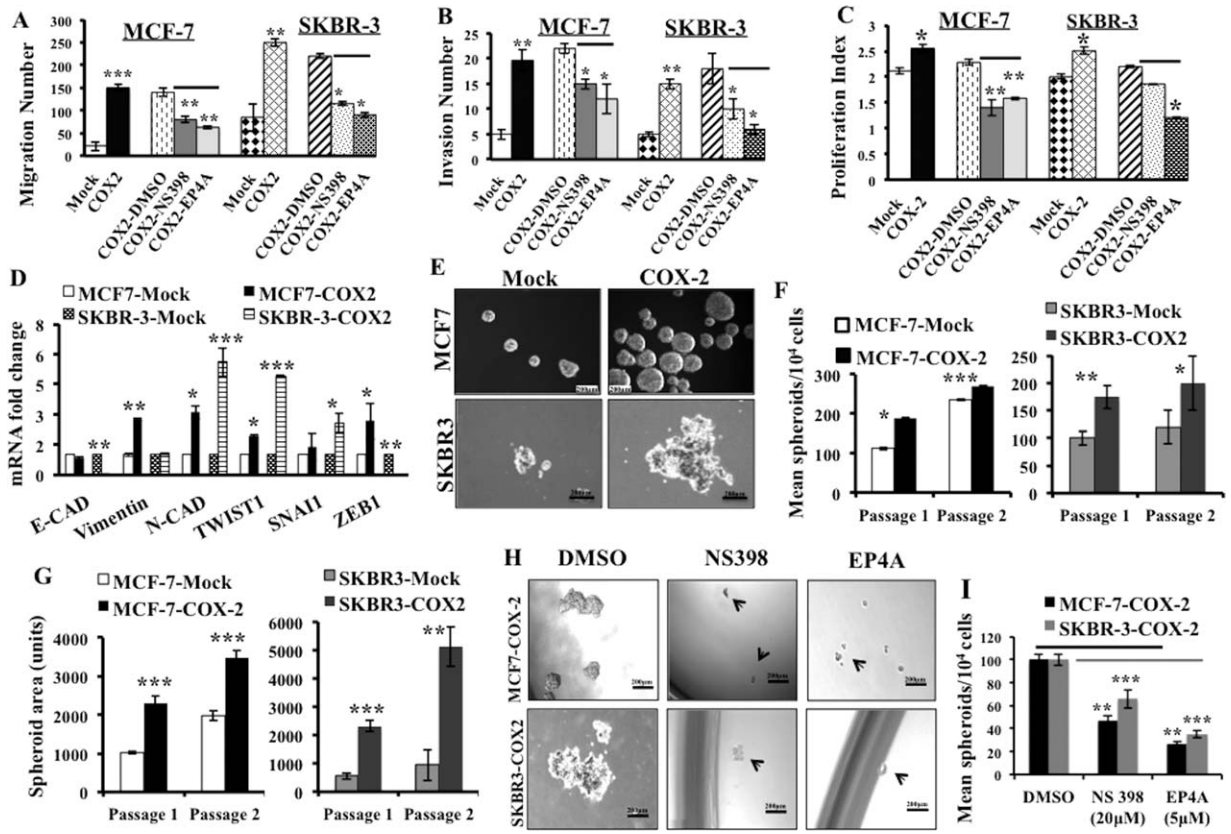

Figure 1. COX-2 over-expression promotes aggressive breast cancer phenotypes: comparison of **(A)** migration, **(B)** invasion, and **(C)** proliferation of Mock and COX-2 over-expressing cells showing enhancement in all phenotypes with COX-2 over-expression. Treatment of COX-2 high cells with NS398 and EP4A (ONO-AE3-208) reverted all phenotypic changes. **(D):** Down-regulation of *E-Cadherin* and up-regulation of *Vimentin, N-Cadherin, TWIST1*, and *SNAIL1* mRNAs in both MCF-7-COX-2 and SKBR-3-COX-2 cells indicates epithelial-mesenchymal transition. *ZEB1* is up-regulated only in MCF-7-COX-2. **(E):** Images of spheroids of both COX-2 over-expressing cells. Increase in stem-like cells (SLC) content in both cell lines shown for successive generations are presented as spheroid number **(F)** and perimeter **(G)**. Treatments with NS398 and EP4A reduced spheroid formation compared to vehicle-treated cells, images in **(H)** and quantified in numbers **(I)**. Scale bar in figures E and H represents 200 μm. The data represent the means of three biological replicates ± SEM. *, $p < .05$; **, $p < .005$; ***, $p < .0005$. All treatments compared with vehicle treatment and all COX-2-over-expressing cells results are compared with Mock-cells.

not show any effect on migration or proliferation of parental cells excluding nonspecific toxicity (Supporting Information Fig. 2A, 2B). Collectively, these results demonstrate that our COX-2 over-expression system recapitulated known COX-2 mediated phenomena in breast cancer cells. We next sought to determine whether COX-2 was associated with increased markers of SLC.

As EMT is associated with SLCs, we explored the effects of COX-2 on this phenomenon. In COX-2 over-expressing cells, mRNA levels of the epithelial marker *E-Cadherin* (*CDH1*) was down-regulated and mesenchymal markers *Vimentin, N-Cadherin, TWIST1*, and *SNAIL* were up-regulated, indicating induction of EMT (Fig. 1D); *ZEB1* was up-regulated only in MCF-7-COX-2 cells.

As a functional correlate, both COX-2 high cell lines showed a significant increase in both the frequency and size (growth rate) of spheroids that persisted for successive generations (images in Fig. 1E, quantitation in Fig. 1F, 1G). Furthermore, these effects of COX-2 on spheroid formation were abrogated when COX-2 overexpressing cells MCF7-COX-2 and SKBR-3-COX2 cells (Fig. 1H, 1I) and also intrinsically COX2 high cells Hs578T cells (Supporting Information Fig. 2C, 2D) were treated with an EP4A or COX-2 inhibitor for 24 hours. However, these treatments had no effect on parental cell lines (Supporting Information Fig. 2E, 2F). These results suggest that SLC induction in COX-2 over-expressing cells is dependent on both COX-2 and EP4 activity.

Expression of stem cell markers in spheroids reflects the presence of SLCs. We observed a preferential colocalization of SLC markers with COX-2 (yellow, shown in inset) in both MCF-7-Mock and MCF-7-COX-2 spheroids (Fig. 2A), consistent with COX-2 induction of SLC phenotype (quantitative data in Supporting Information Fig. 3A). Flow cytometry analysis showed, respectively, 7% and 6% increases in ALDH positive cells in MCF-7-COX-2 (Fig. 2B) and SKBR-3-COX-2 (Fig. 2C) cell lines compared to Mock cell lines. Spheroid formation also increased the incidence of SLC marker (ALDH activity, CD24 and CD44) bearing population in MCF-7 parental and MCF-7-Mock cells (Supporting Information Fig. 4A-4C); this increase was less pronounced in MCF-7-COX-2 cells, which already had a high incidence (Supporting Information Fig. 4D), indicating that COX-2 over-expression on its own increased SLC marker bearing cells. Interestingly, almost all ALDH high cells within MCF-7-COX-2 cells were positively gated for $CD24^+$ and $CD44^+$ (Fig. 2D first two rows), having few or no $CD44^+CD24^-$ subset (lowest row of Fig. 2D).

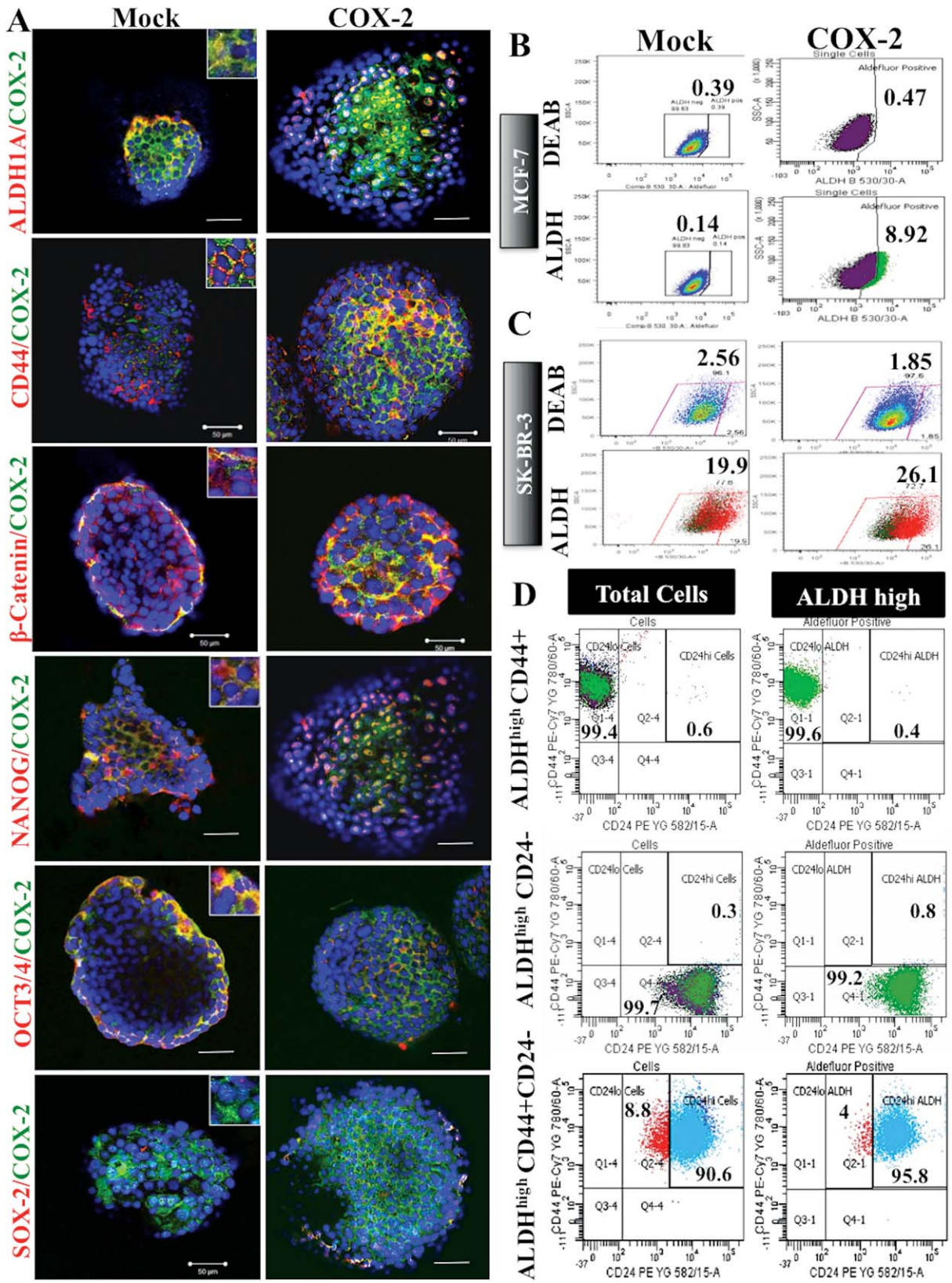

Figure 2. COX-2 over-expression increased SLC contents in breast cancer: **(A)** preferential colocalization of COX-2 and SLC markers in MCF-7-COX-2 spheroids compared to Mock (yellow, shown in inset). FACS analysis showed 7 and 6% increase in ALDH positive cell populations in **(B)** MCF-7-COX-2 and **(C)** SKBR-3-COX-2 cell lines, compared to Mock cell lines, DEAB staining serving as negative control. **(D):** In dual labeled (ALDH-CD44) and (ALDH-CD24) MCF-7-COX-2 cells, more than 95% of ALDH positive cells are positive also for CD44 and CD24. In triple-labeled cells, all ALDH high cells are also positive for both CD44 and CD24; only a small side population of ALDH high cells was low in CD24 and high in CD44. Scale bar in figure (A) represents 50 μm.

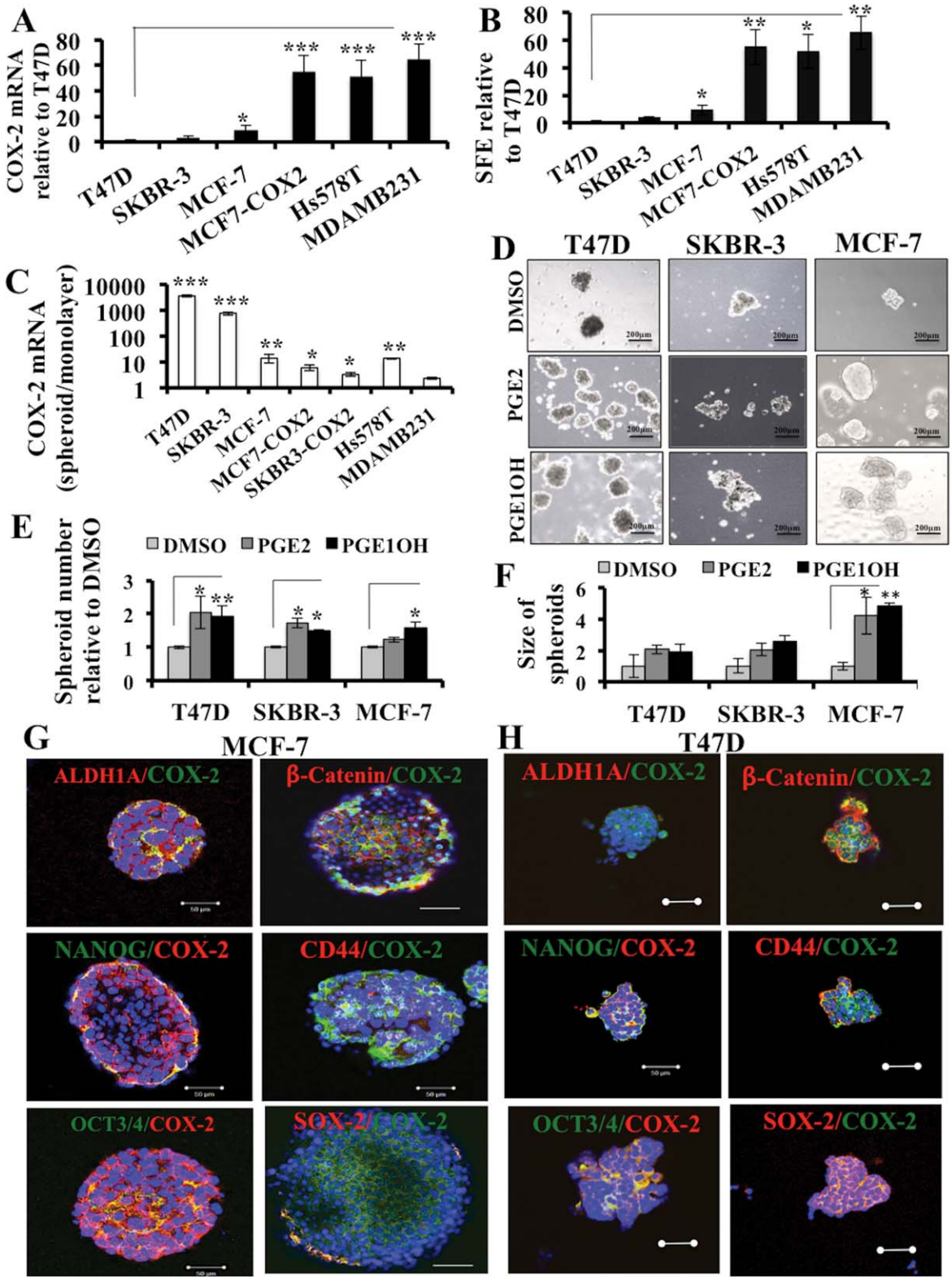

Figure 3. Linking COX-2 and SLCs: mRNA expression in a panel of breast cancer cells showing highest COX-2 expression **(A)** and spheroid formation efficiency (SFE) in COX-2 high cells **(B)**. **(C):** COX-2 expression increased in all cell line-derived spheroids with substantial increase demonstrated in COX-2 low T47D cells, and minimal increases in COX-2 high MDA-MB-231 cells. **(D)** PGE-2 and PGE1OH treatments compared to vehicle treatments increased spheroid formation in T47D, SKBR-3, and MCF-7 cells, shown by spheroid numbers **(E)** and sizes **(F)**. Preferential coexpression of SLC markers and COX-2 (yellow) was noted in **(G)** MCF-7 and **(H)** T47D spheroids after PGE1OH treatment. Scale bar in figure (D) represents 200 μm and in figures (G, H) 50 μm. All experiments replicated three times. The data represent the means biological replicates ± SEM; *, $p < .01$; **, $p < .001$; *** $p < .0001$.

To further explore the possibility that COX-2 may sustain SLCs, we screened human breast cancer cell lines representing luminal (T47D, MCF-7) and basal (SKBR-3, MDA-MB-231, Hs578T) subtypes for COX-2 (*PTGS2*) mRNA expression and tested their spheroid forming efficiency (SFE) [5]. Results showed a parallel between COX-2 mRNA expression (Fig. 3A)

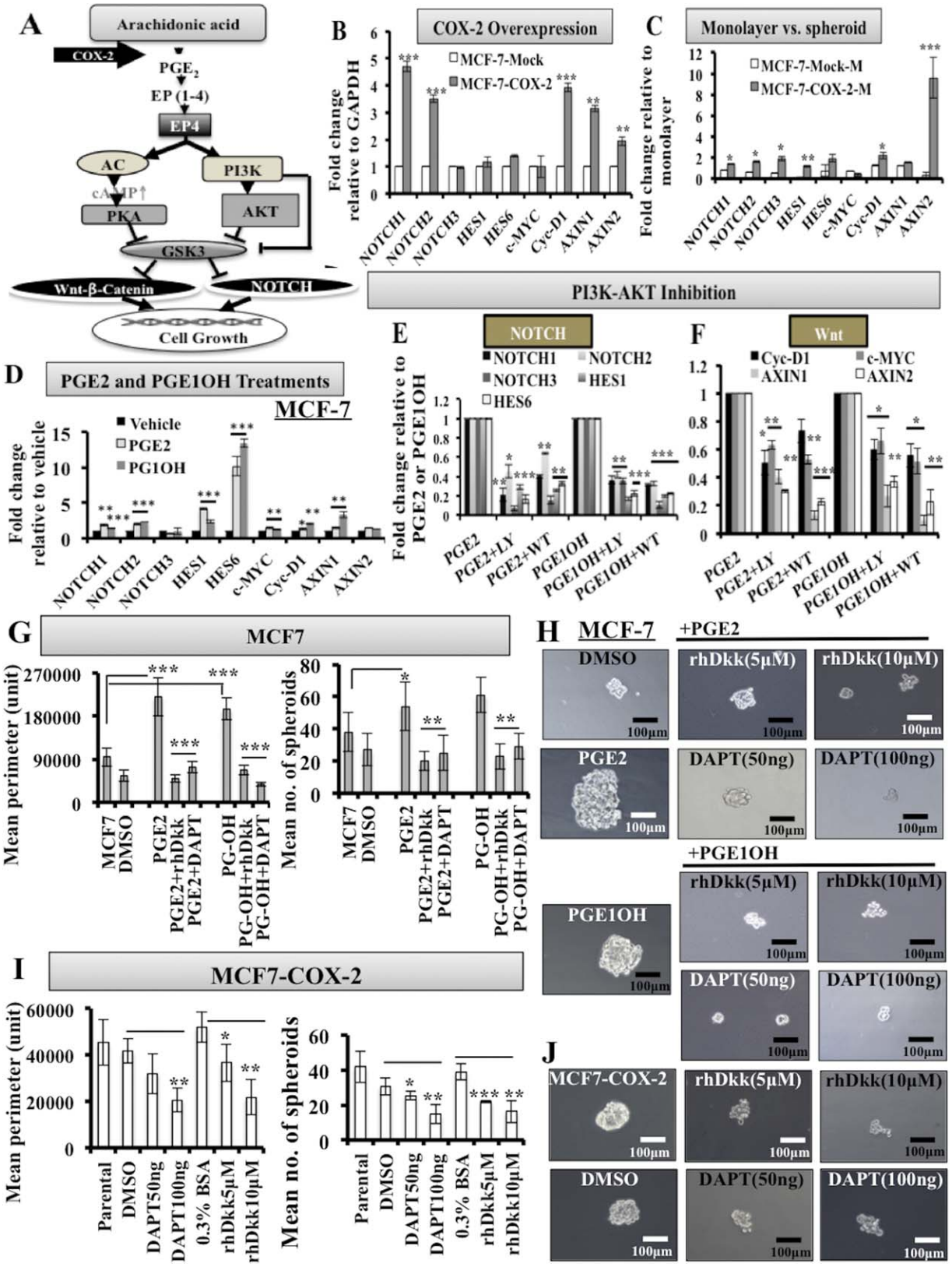

Figure 4.

and SFE (Fig. 3B), both being highest in MCF-7-COX-2 and lowest in T47D. Several studies have shown that spheroid culture enriches for SLCs. Hence, we asked if spheroid formation selects for COX-2 expression in both basal and luminal type breast cancer cells. COX-2 expression increased in all cell lines grown as spheroids relative to monolayers, but the most substantial increase was evident in luminal cells (T47D, MCF-7) having low intrinsic COX-2 expression, and minimal increase was noted in basal cells (MCF-7-COX-2, MDA-MB-231, Hs578T) which exhibited high intrinsic COX-2 expression (Fig. 3C).

Given that prostaglandin receptors (EP)s mediate many of the functions of COX-2, we next investigated the role of EP-receptor activation in SLC induction. We treated COX-2-low cell lines T47D, MCF-7, and SKBR-3 (which produce very low PGE2) with exogenous PGE2 (binding to all EP-receptors) and EP4 agonist PGE1OH (binding selectively to EP4). Both treatments increased spheroid formation nearly to a similar degree (images shown in Fig. 3D; quantification in Fig. 3E, 3F), indicating stimulatory roles of EP receptors in spheroid formation. Preferential coexpression of COX-2 and SLC markers were observed in PGE1OH treated MCF-7 (Fig. 3G) and T47D spheroids (Fig. 3H), quantitative data for T47D provided in Supporting Information Fig. 3B. Collectively, these data suggest that COX-2 induces breast cancer SLCs and that this effect is primarily EP4-dependent.

Differentially Expressed Genes in MCF-7-COX-2 Cells Identified with Microarray. Using mRNA micro-array comparing MCF-7-COX-2 and Mock-transfected cells, restricting our selection to a minimum of $\pm$1.5-fold changes with $p < .05$ (after False Discovery Rate correction), we selected 21 up-regulated genes for further validation and few down-regulated genes (Supporting Information Table 3). Up-regulated genes are *NOTCH1, NOTCH2, AXIN1, WISP1, WNT1*, *CTNNB1*, and *RHOU* genes. We further validated change in NOTCH and WNT pathway genes as described later. Although there are more than 50 genes, which were marginally up-regulated in COX-2 high cells, we selected *ALDH1A*, *CD44*, *NANOG*, *SOX2*, and *POU5F1*, because we observed that these markers were up-regulated in spheroid forming SLCs as well as in tumors in our syngeneic COX-2 expressing murine breast cancer model [5]. Other genes associated with cancer progression (*VEGFA* and *C1QTNF6* linked with angiogenesis, *AMOTL1* and *FGFR4* involving migration), and EMT (masenchymal *SNAI2, CDH2, PCD19*) was also significantly up-regulated. Down-regulated genes included *N1N1* (GSK3beta interacting protein), *PTEN* (negative regulator of PI3K), *PTGFRN* (negative regulator of PGE2 receptor), Cadherin genes (*PCDH9, PCDH20*). These data further supports our observations of the SLC and EMT phenotypes resulting from genetic alterations due to COX-2 over-expression.

Linking NOTCH and WNT Pathways to COX-2/EP4 Induced SLC Function in Breast Cancer. Above results combined with the microarray data led us to hypothesize that COX-2 induces SLC via EP4 activation followed by stimulation of PKA/PI3K/AKT/NOTCH/WNT pathways (schematic diagram presented in Fig. 4A). Both PKA (downstream of EP2/EP4) and PI3K/AKT (downstream of EP4) inhibit GSK3, a negative regulator of WNT/β-catenin and NOTCH, to perpetuate cell proliferation. This hypothesis was also consistent with down-regulation of *NINI* and *PTEN* after COX-2 over-expression. We wanted to test if EP4 activation induces NOTCH and WNT stem cell pathways known to stimulate SLC.

In order to determine whether COX-2 expression is associated with activation of WNT and NOTCH, we measured the aforementioned genes in MCF-7-COX-2 and SKBR-3-COX-2 (relative to respective Mock-transfected) cell lines in monolayer cultures using qRT-PCR. We noted that COX-2 induces a significant increase in *NOTCH1* and *NOTCH2* but minor changes in *NOTCH3, HES1*, and *HES6* mRNA expression in MCF-7-COX-2 cells (Fig. 4B), data for SKBR-3-COX-2 presented in Supporting Information Fig. 5A. MCF-7-COX-2 cells showed significantly increased expression of *WNT* transcription factors *Cyc-D1*, *AXIN1*, and *AXIN2* but no change in *c-Myc* (Fig. 4B), while SKBR-3-COX-2 cells showed no change in the expression of *WNT* genes (Supporting Information Fig. 5A). These data reveal that COX-2 mediates up-regulation of a subset of *NOTCH* and *WNT* family genes.

As spheroid cultures are enriched for SLCs concomitant with COX-2 expression, we next compared *NOTCH* and *WNT* associated gene expression in spheroids versus monolayers. We found that spheroid growth was associated with the stimulation of all *NOTCH* and *WNT* family genes in MCF-7-COX-2 cells except *c-MYC* (Fig. 4C). In SKBR-3-COX-2 cells all *WNT* and *NOTCH* genes were upregulated except *NOTCH1* and *NOTCH3* (Supporting Information Fig. 5B).

Next, we treated COX-2-low cell lines T47D and MCF-7 with 10 μM of PGE2 and PGE1OH and measured expression of *NOTCH* and *WNT* pathway genes. In MCF-7 cells, both treatments effectively increased the expression of all genes except *NOTCH3* and *AXIN2* (Fig. 4D). For T47D, both treatments unregulated selective *NOTCH* and *WNT* pathway genes (Supporting Information Fig. 5C). Thus, COX-2/EP4 mediated SLC induction in human breast cancer cell lines is associated with an up-regulation of *NOTCH* and *WNT*.

Given that EP4 activation leads to the induction of PI3K and that this kinase promotes NOTCH and WNT signaling, we next measured *NOTCH* and *WNT* genes in MCF-7 and T47D cells following PGE2 and PGE1OH treatment in the presence or absence of specific pathway inhibitors: an irreversible PI3K inhibitor Wortmannin (WT), a reversible PI3K inhibitor LY-204002 (LY), or respective vehicles for 24 hours. Since EP4 activation can also stimulate ERK [21] we also used an irreversible ERK inhibitor U0126. Both WT and LY variably

Figure 4. Linking COX-2 and NOTCH and WNT signaling: **(A)** Hypothetical scheme showing EP4 induces SLC via WNT/β-catenin and NOTCH pathways. **(B):** COX-2 over-expression increased *NOTCH1, NOTCH2, Cyc-D1*, *AXIN1*, and *AXIN2* expression in MCF-7-COX-2 cells. **(C):** Spheroid culture condition stimulated both *NOTCH* and *WNT* genes except *c-Myc* and *AXIN1* in MCF-7-COX-2 cells compared to monolayer cells. **(D):** PGE-2 and PGE1OH treatments increased both pathway genes except *NOTCH3* and *AXIN2* in MCF-7. AKT inhibitors LY and WT significantly reduced PGE-2 and PGE1OH induced NOTCH **(E)** and WNT **(F)** signaling in MCF-7. WNT inhibitor rhDkk-1 and NOTCH inhibitor DAPT inhibit PGE-2 and PGE1OH induced spheroid formation of MCF7 (quantification in **G;** image in **H**) and also in MCF-7-COX-2 cells (quantification in **I**; image in **J**). Scale bar in figures (H and J) represents 100 μm. The data represent means of triplicates $\pm$ SEM; compared to Mock transfected or vehicle treated cells. *, $p < .01$; **, $p < .001$; ***, $p < .0001$.

suppressed PGE2 and PGE1OH induced *NOTCH-1/2/3, HES1,* and *HES6* expression and WNT-responsive genes in MCF-7 cells (Fig. 4E, 4F) and T47D cells (Supporting Information Fig. 5E, 5F), but U0126 had little or no effect (data not shown). These data suggest that the EP4-PI3K/AKT axis stimulates *NOTCH* and *WNT* during SLC induction.

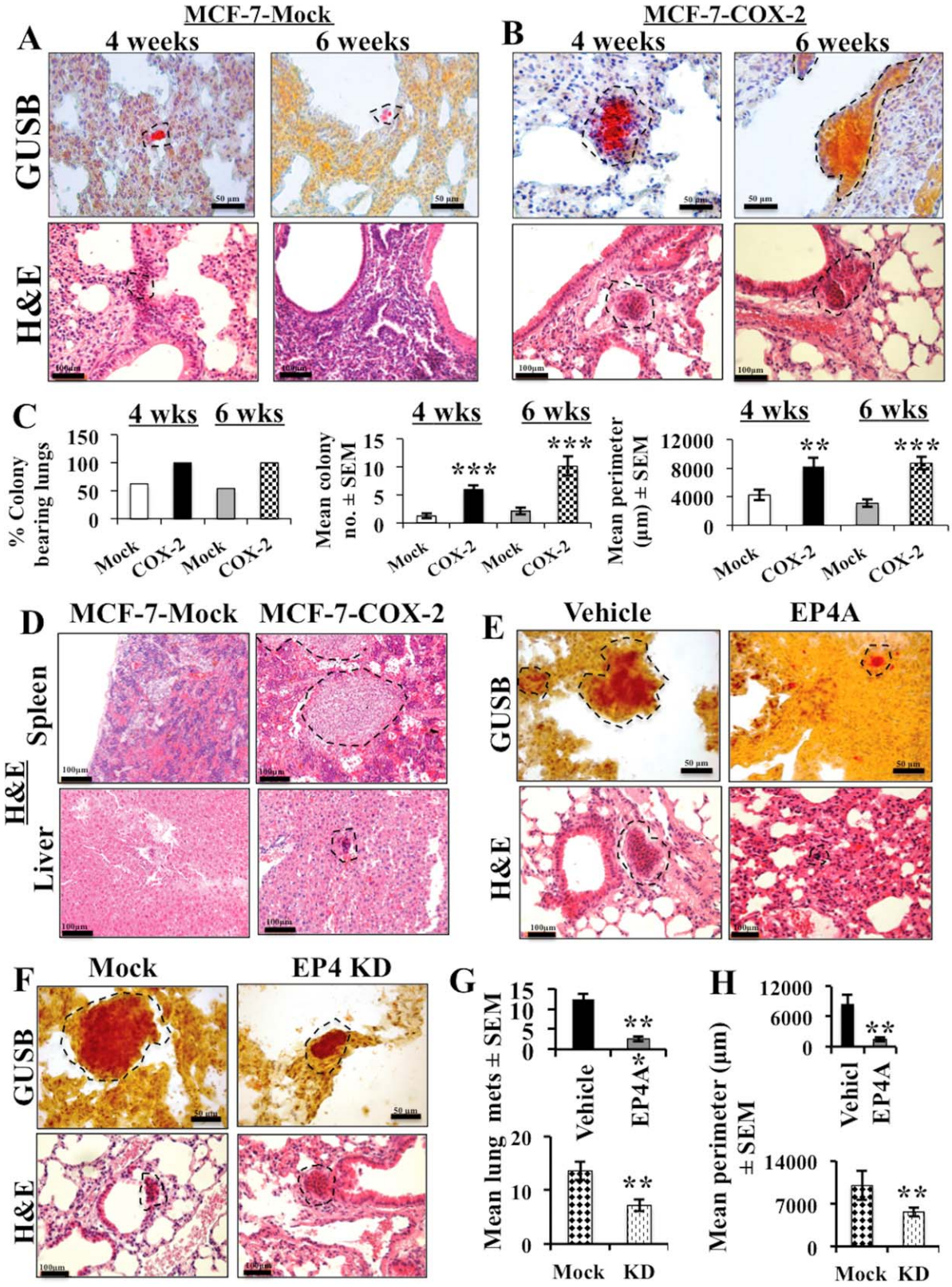

Figure 5.

To show the contribution of NOTCH and WNT pathways in EP4 mediated SLC induction, we used NOTCH and WNT inhibitors DAPT (50 and 100 ng) and rhDkk-1 (5 μM and 10 μM). Both inhibitors significantly reduced PGE2 and PGE1OH stimulated spheroid formation in MCF-7 cells (quantification in Fig. 4G; images in Fig. 4H) and in MCF-7-COX-2 cells (quantification in Fig. 4I; images in Fig. 4J) in a dose dependent manner.

In Vivo Studies

COX-2 Over-Expression Promotes Lung Colony Formation in NOD/SCID/GUSB Null Mice via EP4-Dependent Mechanisms We previously showed that inhibiting COX-2 or EP4 activity reduced the growth of COX-2 expressing murine C3L5 primary breast carcinomas and their spontaneous metastases in vivo [5, 18]. In this study, we injected MCF-7-Mock and MCF-7-COX-2 cells into the tail vein of GUSB null/NOD/SCID mice and euthanized them at 4 and 6 weeks to quantify lung colonies with GUSB staining (red, marking donor cells) and metastases in other organs We selected a minimum of three subserial coronal sections of lungs in each mouse to represent the largest surface area to score metastatic foci. For other organs we scanned a minimum of five sections of each organ per mouse. Morphological data are presented in Fig. 5A, 5B. The incidence of lung-metastasis-bearing mice among the mice injected with tumor cells and the incidence of metastatic foci per lung in those bearing metastases are shown in Fig. 5C. Both parameters were significantly higher in mice injected with MCF-7-COX-2 cells, as compared to MCF-7-Mock cells. Metastatic colonies in the spleen and liver were also recorded with MCF-7-COX-2 cells (Fig. 5D).

To investigate the contribution of EP4 in lung colonization, we stably knocked-down EP4 in MCF-7-COX-2 cell line (named as MCF-7-COX-2-EP4KD, Supporting Information Fig. 6A) or treated MCF-7-COX-2 cells with EP4A (5 μM) for 7 days in vitro before tail vein injection. EP4A treatment (morphology in Fig. 5E) and EP4 knock-down (morphology in Fig. 5F) in MCF-7-COX-2 cells reduced both the lung colony numbers (Fig. 5G) and colony sizes (Fig. 5H).

Mammary Site Transplantation of MCF-7-COX-2 Cells Promotes Tumor Growth and Spontaneous Metastasis in NOD/SCID/IL2Rγ Null Mice. Mammary transplants of MCF-7-COX-2 cells were carried out in NOD/SCID/IL2Rϒ null mice rather than NOD/SCID/GUSB null mice because the former strain lacks functional T/B/NK cells accepting better xenotransplants.

In first generation (F1) transplants, tumor takes (incidence) and growth were significantly higher with MCF-7-COX-2 cells compared to MCF-7-Mock cells at respective inoculum doses (Fig. 6A). On days 73-75, excised tumors were re-transplanted in another set of mice at lower inoculum doses (5×10^4 and 5×10^3 cells), called generation F2. Tumor take with MCF-7-COX-2 cells was 100% in both F1 and F2 (Fig. 6B). For MCF-7-Mock cells the incidences were 60%-80% in F1 and only 30% in F2 (Fig. 6B). MCF-7-Mock tumors remained avascular and grew poorly, whereas MCF-7-COX-2 transplants grew larger and were vascular (Fig. 6C).

We next sought to determine if spontaneous metastasis was affected by COX-2 expression. HLA staining for human-derived cells confirmed spontaneous lung metastasis in mice bearing both F1 and F2 MCF-7-COX-2 tumors (Fig. 6D). Lung metastases arising from COX-2 and Mock cells were enumerated and data are presented as the number of lung colonies (>8 cells) and clusters (2-8 cells) in Fig. 6E. Representative images of clusters (<8 cells) are presented in Supporting Information Fig. 6B-4G. Even with H&E staining (Fig. 6F), we identified spontaneous metastatic colonies in the lungs, spleen and liver of all MCF-7-COX-2 tumor-bearing mice in F1 (100%), whereas only one mouse bearing MCF-7-Mock tumor displayed clusters in the spleen and liver (12.5%) and two mice showed lung colonies (25%).

To determine SLC frequencies within tumors, cell lines derived from MCF-7-Mock and MCF-7-COX-2 tumors were named MCF-7-Mock-T and MCF-7-COX-2-T respectively. Both cell lines showed accelerated ability to form very large spheroids (>60 μm diameter) as early as day 3 (image and quantitation in Supporting Information Fig. 7A-7C), compared to 7-12 days required by MCF-7 cells to grow spheroids of that size [19]. We noted a dramatic increase in COX-2-positive cells in both cell line spheroids, indicating a selection in vivo (Supporting Information Fig. 7D). Double immune-staining for COX-2 and SLC markers (ALDH1A, CD24, CD44, β-Catenin and SOX-2) in spheroids revealed higher incidence of cells co-expressing COX-2 with ALDH1A, CD44 and β-Catenin in MCF-7-COX-2-T spheroids than in MCF-7-Mock-T spheroids, which displayed high CD24 and β-Catenin coexpression (quantitative data not provided).

We next wanted to determine if COX-2 induced phenomena, such as EMT and expression of proangiogenic/lymphangiogenic factors observed in vitro, were recapitulated in the tumors. We quantified *EP4, VEGF-C/D, LYVE-1, CD31*, and *E-Cadherin/Vimentin* mRNA with Taqman gene expression assays in tumors extracted from F1. MCF-7-COX-2 tumors showed significant up-regulation of *EP4,* angiogenesis and lymphangiogenesis markers *VEGF-C/D, LYVE-1/CD31* and masenchymal marker *Vimentin* and down-regulation of epithelial marker E-Cadherin (*CDH1*) compared to MCF-7-Mock tumors (Supporting Information Fig. 8). We could not retrieve enough tissue from F2 tumors to extract RNA. These patterns also occurred at the protein level (Fig. 6G). Angiogenic and lymphangiogenic

Figure 5. COX-2 over-expression promotes the incidence and growth of micrometastases: GUSB staining (marking donor cells, red) showing pulmonary micro-metastases following intravenous injections of **(A)** MCF-7-Mock and **(B)** MCF-7-COX-2 cells at 4 weeks and 6 weeks. H&E staining presented in the bottom panel. **(C):** Incidence of colony bearing lungs, mean colony numbers and sizes (perimeters) in mice injected with MCF-7-COX-2 cells are higher compared to mice injected with MCF-7-Mock at both the time points. **(D):** H&E staining of liver and spleen confirmed metastatic colonies in mice bearing MCF-7-COX-2. **(E):** EP4A treatment of MCF-7-COX-2 cells with ONO-AE3208 (5 μM for 7 days) before injection or **(F)** EP4 knock-down (KD) in MCF-7-COX-2 cells reduced lung colony formation compared to mock transfected or vehicle treated cells. For both assays, reduction in lung colony numbers and sizes are presented in **(G)** and **(H)** respectively. Scale bar in figures (A), (B), (E), and (F) in GUSB staining pictures represents 50 μm and H&E staining pictures in (A), (B), (D), (E), and (F) represents 100 μm. The data represent means (8 mice per condition × 3 sections per lung. $n = 24$) ± SEM. *, $p < .05$; **, $p < .005$; ***, $p < .0005$.

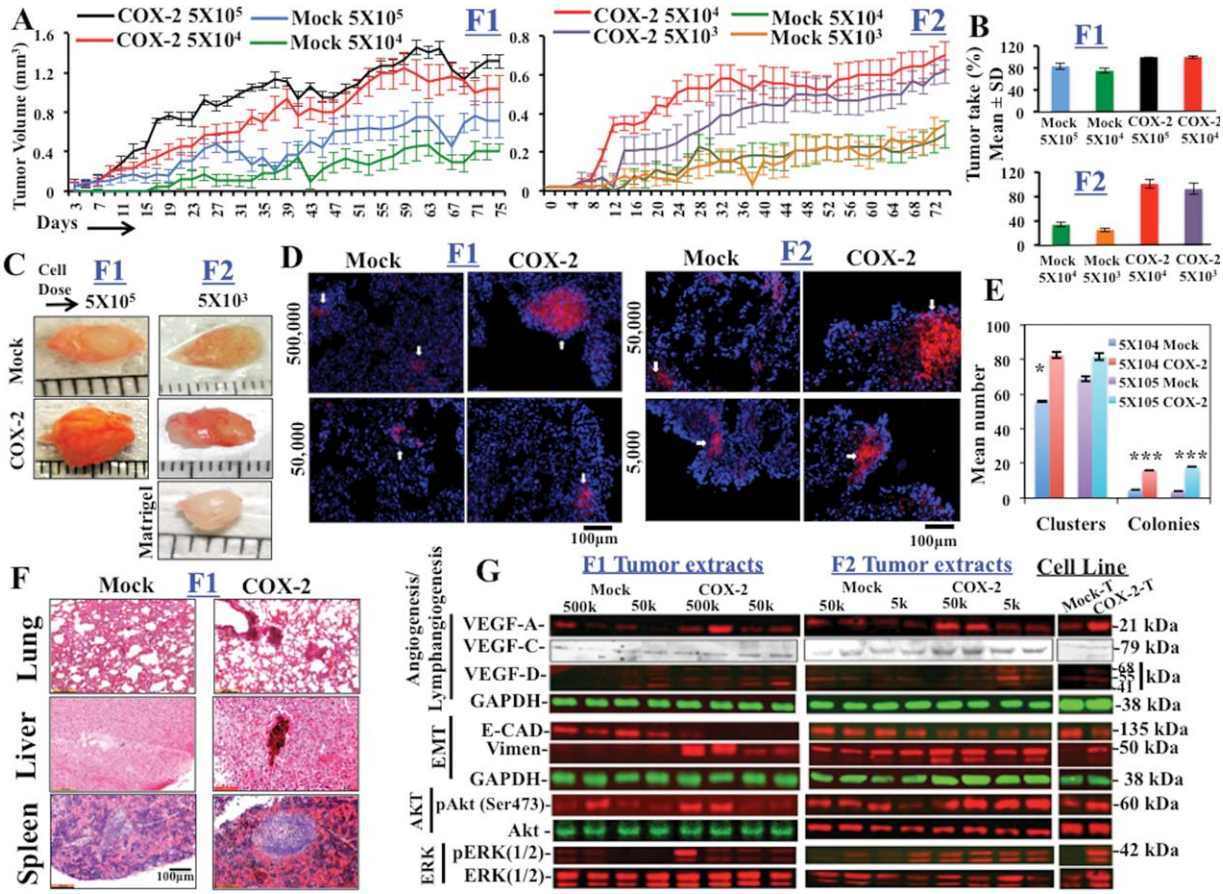

Figure 6. MCF-7-Mock and MCF-7-COX-2 cells transplanted in NOD/SCID/IL-2Rγ null mice, 4 mice per dose of cells transplanted at four points, $n = 16$. **(A):** Tumor growth was evidently high with MCF-7-COX-2 transplants compared to MCF-7-Mock in both F1 (primary transplants) and F2 (secondary transplants). **(B):** Tumor take was 100% for MCF-7-COX-2 transplants in both experiments while for Mock it goes down from 60%-80% in F1 to 20%-30% in F2 transplants. **(C):** Pictures showing larger tumors with increased vasculature in COX-2 transplants compared to Mock. Matrigel implants served as negative control. **(D):** Spontaneous metastasis to lungs was confirmed by human HLA staining, quantitation presented in **(E)**, data presented as mean (4 mice per condition X 4 lungs X 3 sections per lung, $n = 48$) ± SEM. *, $p < .05$; **, $p < .005$; ***, $p < .0005$. **(F):** MCF-7-COX-2 implants produced secondary metastasis in liver and spleen, shown by H&E staining. Scale bar in figures D and F represents 100 μm. **(G):** Western blot analysis of F1 and F2 tumor lysates (pooled from 8 tumors per group, triplicate measurements, shown in duplicate) and F1-tumor derived cell lines MCF-7-Mock-T and MCF-7-COX-2-T lysates. In F1, VEGF-A, C, D, Vimentin, pAKT and pERK expressions were higher compared to MCF-7-Mock lysates; in contrast E-Cadherin expression went down. In all F2 tumors expression of all markers increased compared to F1. MCF-7-COX-2-T cell line showed higher expression of all markers and down-regulation of E-Cadherin compared to MCF-7-Mock-T cells.

proteins (VEGF-C and VEGF-D) and mesenchymal protein (Vimentin) were up-regulated and epithelial marker E-Cadherin down-regulated in MCF-7-COX-2 tumors as compared to MCF-7-Mock tumors in both F1 and F2. Similar alterations were also observed in F1 derived tumor cell lines MCF-7-Mock-T and MCF-7-COX-2-T (Fig. 6G). Finally, we determined PI3K/AKT and/or ERK1/2 phosphorylation in all cell lines and tumor lysates of F1 and F2. Over-expression of COX-2 increased phosphorylation of both AKT and ERK in cell lines and tumors in all conditions tested. All images are presented in Fig. 6G and quantification presented in Supporting Information Fig. 9.

In Situ Studies

COX-2, EP2, EP4, and SLC Marker Expression Levels in Primary Human Breast Cancer. We quantified *COX-2* (Fig. 7A), *EP2* (Fig. 7B), *EP4* (Fig. 7C), *ALDH1A* (Fig. 7D) mRNA expression in a panel of human breast cancer ($n = 105$) and adjacent nontumor ($n = 20$) tissues. RNA extraction and cDNA synthesis were performed as described previously [19]. Data expressed as delta Ct (lower delta Ct indicate higher expression), revealed significantly higher expression of all markers in tumor than nontumor tissues. The mean of delta Ct values of three control genes *GAPDH, β-actin* and *RLP5* were used to normalize mRNA expression. Strong positive correlation is noted between *COX-2/EP4* (Fig. 7E), *EP4/ALDH1A* (Fig. 7F) and *COX-2/ALDH1A* (Fig. 7G) in breast cancer tissues. *COX-2* and to some extent, *EP2* and *EP4* expression increased with the stage of cancer. *ALDH1A* was expressed at all stages, the highest expression observed in stage IV (Fig. 7H).

In situ immunofluorescence staining of breast cancer tissue sections ($n = 10$), revealed colocalization of ALDH, SOX2, OCT3/4, NANOG, and CD44 in a subpopulation of COX-2 positive cells (Fig. 7I).

Survival analysis was done with data extracted from human cancer genome atlas [41]. Results revealed that high expression of *COX-2* (Fig. 7J) and *EP4* (Fig. 7K) genes was associated with reduced patient survival.

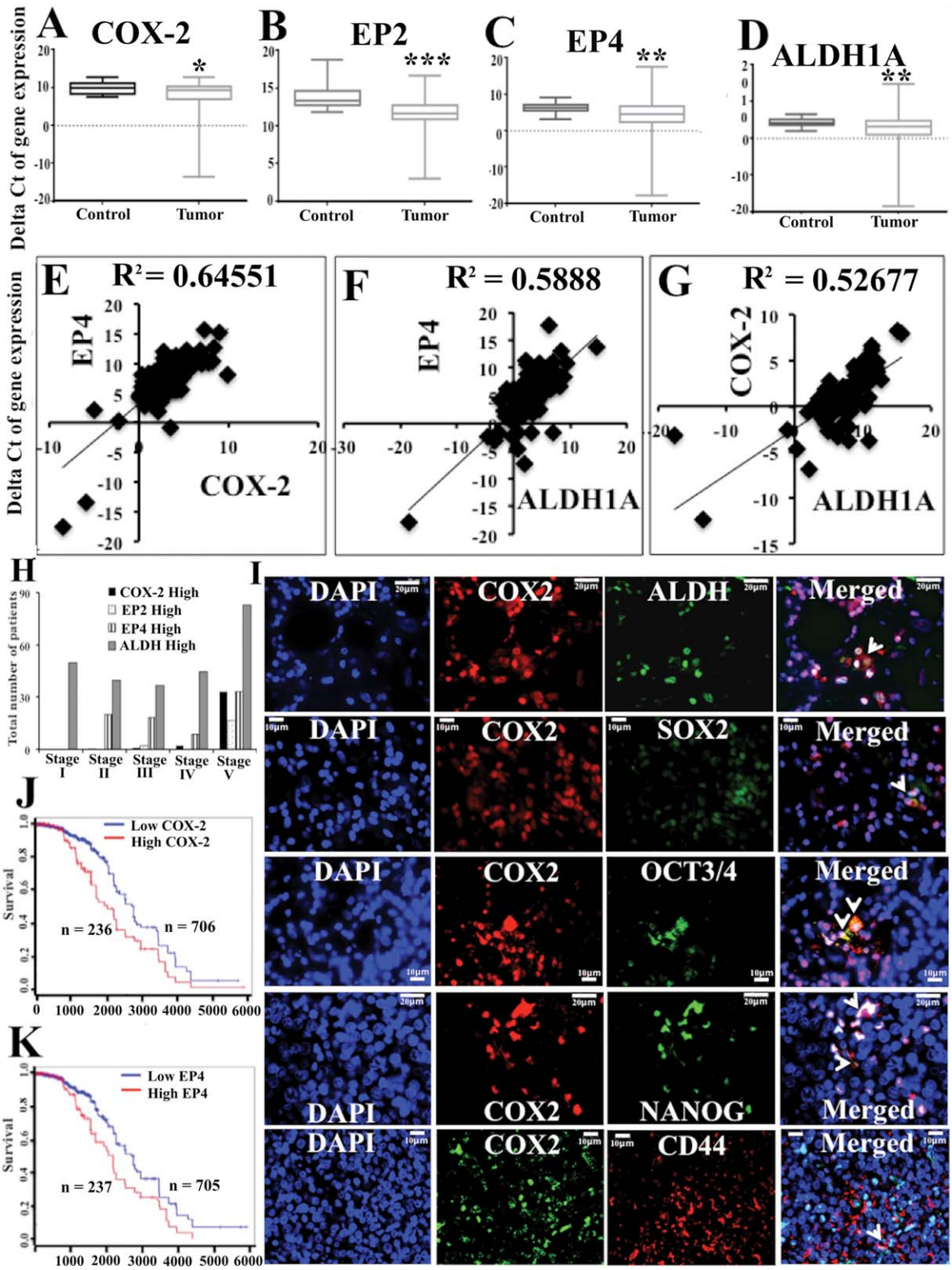

Figure 7. Box-and-whisker plot showing over-expression of **(A)** *COX-2*, **(B)** *EP2*, **(C)** *EP4*, and **(D)** *ALDH1A* mRNA in primary human breast tumors ($n = 105$), in comparison to nontumor control tissue ($n = 20$). A more negative ΔCt value indicates a higher mRNA expression level. Strong positive correlation existed between **(E)** *COX-2/EP4*, **(F)** *EP4/ALDH1A*, and **(G)** *COX-2/ALDH1A* in patient population. Data presented as mean of $n = 105$ for tumor and $n = 20$ for control tissue. **(H):** *COX-2, EP2, EP4*, and *ALDH1A* expression were the highest in stage IV. **(I):** Double immune staining of COX-2 and SLC markers in breast tissue sections (yellow) showing co-localization of ALDH, SOX2, OCT3/4, NANOG, and CD44 with COX-2. In figure (I), images with NANOG and ALDH scale bar represents 20 μm and in images with SOX2, OCT3/4, and CD44 scale bar represents 10 μm. Data mining results showing high expression of **(J)** *COX-2* and **(K)** *EP4* is associated with reduced patient survival.; *, $p < .05$; **, $p < .01$; ***, $p < .005$.

Discussion

In the present study, we demonstrate the stimulatory roles of COX-2 and EP4 in human breast cancer progression and SLC induction via PI3K/AKT/NOTCH and WNT pathways, combining in vitro, in vivo, and in situ approaches. This work supports our previous studies, wherein we showed SLC stimulatory roles of COX-2 and EP4 in a murine breast cancer model [5]. The role of COX-2 in SLC induction has been hypothesized [42] and the roles of EP4 documented in human breast cancer cells [43]. We reported that COX-2/EP4 mediated induction of an oncogenic microRNA-526b was linked with SLC stimulation [19]. However, the mechanisms underlying COX-2/EP4 mediated SLC induction in human breast cancer remained unclear. In the present study, for the first time, we identified the mechanistic roles of COX-2/EP4 in SLC induction in human breast cancer, proposing a linear activation of COX-2, EP4, PI3K/AKT leading to up-regulation/activation of NOTCH and WNT pathways (Schema presented in Fig. 4A), which are SLC-linked.

Multiple approaches adopted in our study were corroborative in nature. Our findings of a positive correlation of COX-2 expression with spheroid forming ability in genetically disparate human breast cancer cell lines (Fig. 3) suggested that COX-2 may stimulate SLCs irrespective of breast cancer genotype. This contention was validated by the phenotypic changes resulting from ectopic COX-2 over-expression in COX-2 low HER2+/− cell lines. Our in situ studies of genetically heterogeneous human breast cancer tissue mRNA, showing a positive correlation of COX-2 and EP4 with the SLC marker ALDH reinforces this view. In further support, we noted an association of immune-stained SLC markers with COX-2 in breast cancer cells in situ.

Several studies including ours have reported the contribution of EP4 receptor on tumor cells [5, 18, 42] as well a host cells such as NK cells [44] and macrophages [5] in murine breast cancer progression. Activation of PKA pathway shared by EP2 and EP4 [22] was identified as one of the mechanisms in COX-2 mediated SLC stimulation [19]. EP4 activation can also stimulate ERK [45] and PI3K/AKT [46] pathways, respectively, promoting PGE-2 dependent cell survival [46] and migration [47]. In our murine C3L5 breast cancer model, therapy with EP4 antagonists inhibited tumor growth and metastasis to lymph nodes and the lungs, and residual tumors exhibited reduced AKT phosphorylation, indicating EP4 inactivation [5, 18]. Furthermore, EP4A therapy exhibited a distinct SLC-reductive effect, as noted from the reduction of multiple SLC marker bearing cells in residual tumors [5]. In the present study, the roles of EP4 receptor in COX-2 mediated aggressive functions and SLC induction in human breast cancer were demonstrated with multiple approaches: (a) stimulation of all aggressive breast cancer functions in vitro could be blocked with COX-2 inhibitors as well as EP4 antagonists. (b) Pretreatment of MCF-7-COX-2 cells with an EP4 antagonist or EP4 knock-down of the cells reduced their lung colony forming ability in vivo. (c) EP4 activation in vivo was indicated by increased AKT and ERK phosphorylation in serial xenotransplants. (d) EP4 activation in multiple COX-2 low cells with an EP4 agonist promoted SLC phenotype as shown by increased spheroid forming efficiency and the incidence of SLC-marker bearing cells. (e) Concomitantly there was up-regulation of certain genes in NOTCH and WNT family, which could be blocked by inhibiting the PI3K/AKT pathway, unique to EP4 activation, not shared by EP2 [22]. However, our studies did not exclude the roles of cAMP-PKA pathways shared by EP2 and EP4. Indeed, PGE-2 mediated SLC stimulation noted in our study could be in part due to EP2 activation. In our COX-2 expressing murine breast cancer model we have excluded the role of EP1 in tumor growth and metastasis [18]. (f) EP4 mediated SLC induction was shown to be dependent on NOTCH and WNT activation. (g) A positive association of EP4 mRNA expression with SLC marker ALDH1A was noted in human primary breast cancer tissues, and high EP4 expression was associated with reduced survival.

Activation of NOTCH [48] and WNT [49] pathways has been shown for cell renewal and cell fate determination in human embryonic stem cells. Both NOTCH [26, 27] and WNT [28, 29] pathways were reported to be activated in breast cancer, promoting metastatic phenotype. Furthermore a small molecule inhibitor of WNT/β catenin was shown to be SLC-reductive in breast cancer cells [50]. PGE-2, the major bioactive product of the COX-2 cascade can protect embryonic stem cells [51] and activate components of the WNT signaling system [31]. In this study, we observed an up-regulation of NOTCH and WNT signaling genes following ectopic COX-2 expression or treating COX-2 low T47D and MCF-7 cells with the nonselective EP ligand PGE-2 or a selective EP4 agonist PGE1OH. These treatments also promoted spheroid formation. Furthermore, PGE-2 and PGE1OH mediated up-regulation of NOTCH and WNT was blocked with selective P13K-AKT inhibitors. NOTCH and WNT inhibitors could also block COX-2/EP4 induced spheroid formation. Thus, for the first time we have shown that EP4 receptor activity, via PI3K/AKT signaling followed by NOTCH/WNT up-regulation/activation plays a role in COX-2 mediated SLC induction.

Conventional tumor growth assays using histology and/or whole animal imaging do not permit the single cell resolution that we uncovered with the GUSB-null mouse model. COX-2 over-expressing cells injected intravenously in these mice formed micrometastasis in the lungs at 4 weeks, progressing to macrometastases by 6 weeks, at which time the mice showed multiorgan metastases. In contrast, the Mock cells were identified either as single cell or small clusters in the lungs, which never progressed to micro-metastases even at 6 weeks, indicating that COX-2 over-expression may promote growth of dormant cells. This view was supported by the fact that few or no EdU positive cells were noted in the lungs of MCF-7-Mock injected mice, whereas colonies in MCF-7-COX-2 injected mice revealed high incidence of EdU positive cells (Supporting Information Fig. 10).

Demonstration of SLC properties by single cell transplantation is hard in the case of solid tumors because of cellular heterogeneity, in which case SLC phenotype in vitro, combined with tumorigenicity with small cell numbers in serial transplants expressing SLC-associated markers have been useful [3, 36]. In the present study, we observed that COX-2 over-expression leads to an enrichment of $ALDH^{high}CD44^{+}CD24^{+}$ cells in association with increased spheroid forming efficiency, we could not however identify a subset which is $ALDH^{high}CD44^{+}CD24^{-}$. It is possible that COX-2 induced SLC phenotype does not necessarily deplete CD24 positive cells. In spheroid derived cells ALDH, CD44, and CD24 positive cells was more evident for COX-2 low MCF-7, than MCF-7-COX-2 cells, likely because spheroid formation leads to increased COX-2 expression in COX-2 low cell lines (Fig. 3A, 3B). COX-2

association with SLC in vivo was further demonstrated by serial transplantation. We observed aggressive growth of implants at the mammary sites in IL2Rγ null mice with 5×10^4 MCF-7-COX-2 cells in the first generation and only 5×10^3 MCF-7-COX-2 tumor dissociated cells in the second generation, indicating the role of COX-2 in SLC selection in vivo. This inference was further supported by enrichment of SLC-marker bearing cells co-expressing COX-2 in tumor-derived spheroids.

Metastatic tumor cells can survive at secondary sites in the body circumventing a need for growth or progression, a property called tumor dormancy [52]. In the present study, using HLA marker, we observed spontaneous lung colonies and clusters of MCF-7-COX-2 in cells seeding from mammary site transplants in IL2Rγ null mice. In MCF-7-Mock transplants we never found spontaneous lung colonies, whereas occasional single cells were noted indicating metastatic cells that remained dormant. These findings were also reproduced in second-generation transplants, reinforcing the role of COX-2 in abrogation of tumor dormancy.

Significant up-regulation of the VEGF family members and angiogenesis and lymphangiogenesis markers in MCF-7-COX-2 derived tumors relative to MCF-7-Mock tumors further support the stimulatory roles of COX-2 in angiogenesis and lymphangiogenesis, already demonstrated in our murine breast cancer model [5, 18]. This also applied to increased AKT and ERK activation in MCF-7-COX-2 tumors in vivo, as demonstrated in the murine breast cancer model [5, 18] reinforcing the role of EP4 activity in COX-2 mediated tumor progression.

We suggest that COX-2 and EP4 are both partners in SLC induction in breast cancer. This suggestion is supported by (a) a reduction in spheroid formation with COX-2 inhibition; (b) EP4 antagonism or gene knock-down reducing lung colonies in vivo; (c) a strongly positive correlation of *COX-2/EP4* mRNA with breast cancer stem cell marker *ALDH1A* in tumor tissues; (d) preferential colocalization of immunostained SLC markers with COX-2 in breast tumor tissues.

Our studies in the human, for the first time demonstrate the role of EP4, and EP4 mediated signaling pathways in COX-2 mediated human breast cancer progression including SLC stimulation. While COX-2 inhibitors have demonstrated proven chemo-preventive and therapeutic effects in numerous epithelial-derived cancers [13] cardiovascular side effects of COX-2 inhibitors [23] resulting from inhibition of cardio-protective prostanoids such as PGI2 [25] demonstrate the need for alternate safe targets downstream of COX-2. We suggest that EP4 exquisitely meets this need. We have already shown in our preclinical studies the efficacy of EP4 antagonists in blocking multiple COX2/EP4 mediated mechanisms in breast cancer progression including SLC reduction [5]. Based on the evidence of multiple roles of EP4 on tumor and host cell mediated mechanisms in breast cancer progression, we suggest that testing the use of EP4 antagonists as adjuvant in human breast cancer is appropriate and timely.

Acknowledgments

This study was supported by grants of the Ontario Institute of Cancer research and Canadian Breast Cancer Foundation, Ontario chapter to PKL, Translational Breast Cancer Research Unit Postdoctoral Fellowship (funded by the Breast Cancer Society of Canada) to MM. MM and MR are fellows of the Canadian Institutes of Health Research Strategic Training Program in Cancer Research and Technology Transfer (CIHR-CaRTT). KMV and MR hold Vanier Canada graduate scholarships. We thank Dr. Takayuki Maruyama of Ono Pharmaceutical, Osaka, Japan for providing us ONO-AE3-208. We thank Qian Xing, Claire kwon and Jose Torres-Garcia for technical help and Gillian Bell for tail vein injections in mice. We highly appreciate Aya Abdou to screen tediously all lung colonies of NOD/SCID mice and Andrew Deweyer for quantifying spheroid formation efficiency with NOTCH WNT inhibitors.

Author Contributions

M.M.: Conception and design, collection and/or assembly of data, data analysis and interpretation, manuscript writing, other (mentoring students to conduct experiments and troubleshooting); X.X.: Collection and/or assembly of data; L.L.: Collection and/or assembly of data; E.T.-F.: Collection and/or assembly of data, other (proof reading of the article); M.R.-T.: Collection and/or assembly of data; K.V.: Collection and/or assembly of data, survival data analysis; L.-M.P.: Conception and design, final approval of the manuscript; D.H.: Provision of study material (NOD/SCID mice), other (in vivo experiment designing and troubleshooting); P.K.L.: Conception and design, financial support, administrative support, provision of study material, manuscript writing, final approval of the manuscript.

Potential Conflicts of Interest

All authors declared no potential conflicts of interest.

References

1 American Cancer Society. Cancer Facts & Figures 2014. Atlanta: American Cancer Society; 2014.

2 Nahta R, Shabaya S, Ozbay T et al. Personalizing HER2-targeted therapy in metastatic breast cancer beyond HER2 status: What we have learned from clinical specimens. Curr Pharmacogenomics Person Med 2009;7:263–274.

3 Wicha M, Liu S, Dontu G. Cancer stem cells: an old idea – a paradigm shift. Cancer Res 2006;66:1883–1890.

4 Luo W, Li S, Peng B et al. Embryonic stem cells markers SOX2, OCT4 and Nanog expression and their correlations with epithelial-mesenchymal transition in nasopharyngeal carcinoma. PLoS One 2013;8:e56324. doi: 10.1371/journal.pone.0056324.

5 Majumder M, Xin X, Liu L et al. EP4 as the common target on cancer cells and macrophages to abolish angiogenesis, lymphangiogenesis, metastasis and SLC functions. Cancer Sci 2014;105:1142–1151. doi: 10.1111/cas.12475.

6 Al-Hajj M, Wicha MS, Benito-Hernandez A et al. Prospective identification tumorigenic breast cancer cells. Proc Natl Acad Sci USA 2003;100:3983–3988. doi: 10.1073/pnas.0530291100.

7 Hwang WL, Yang MH, Tsai ML et al. SNAIL regulates interleukin-8 expression, stem cell-like activity, and tumorigenicity of human colorectal carcinoma cells. Gastroenterology 2011;141:279–291, 291.e1-5. doi: 10.1053/j.gastro.2011.

8 Vesuna F, Lisok A, Kimble B et al. Twist modulates breast cancer stem cells by transcriptional regulation of CD24 expression. Neoplasia 2009;11:1318–1328.

9 Chaffer CL, Marjanovic ND, Lee T et al. Poised chromatin at the ZEB1 promoter enables breast cancer cell plasticity and enhances tumorigenicity. Cell 2013;154:61–74. doi: 10.1016/j.cell.2013.06.005.

10 William CS, Moss M, Dubois RN. The role of cyclooxygenases in inflammation, can-

cer, and development. Oncogene 1999;18: 7908–7916.
11 Subbaramaiah K, Dannenberg AJ. Cyclooxygenase 2: a molecular target for cancer prevention and treatment. Trends Pharmacol Sci 2003;24:96–102.
12 Harris RE, Beebe-Donk J, Alshafie GA. Reduction in the risk of human breast cancer by selective cyclooxygenase-2 (COX-2) inhibitors. BMC Cancer 2006;6:27.
13 Ristimaki A, Sivula A, Lundin J et al. Prognostic significance of elevated cyclooxygenase-2 expression in breast cancer. Cancer Res 2002;62:632–635.
14 Lala PK, Parhar RS, Singh P. Indomethacin-therapy abrogates in prostaglandin-mediated suppression of natural killer activity in tumor bearing mice and prevents tumor metastasis. Cell Immunol 1986;99: 108–118.
15 Rozic J, Chakraborty C, Lala PK. Cyclooxygenase inhibitors retard murine mammary tumor progression by reducing tumor cell migration, invasiveness and angiogenesis. Int J Cancer 2001;93:497–506.
16 Timoshenko A, Xu G, Chakrabarti S et al. Role of prostaglandin E2 receptors in migration of murine and human breast cancer cells. Exp Cell Res 2003;289:265–274.
17 Timoshenko A, Chakraborty C, Wagner G et al. COX-2-mediated upregulation of the lymphangiogenic factor VEGF-C in human breast cancer. Br J Cancer 2006;94:1154–1163.
18 Xin X, Majumder M, Girish GV et al. Targeting COX-2 and EP4 to control tumor growth, angiogenesis, lymphangiogenesis and metastasis to the lungs and lymph nodes in a breast cancer model. Lab Invest 2012;92: 1115–1128. doi: 10.1038/labinvest.2012.90.
19 Majumder M, Landman E, Liu L et al. COX-2 elevates oncogenic miR-526b in breast cancer by EP4 activation. Mol Cancer Res 2015;13:1022–1033. doi: 10.1158/1541-7786 MCR-14-0543
20 Breyer RM, Bagdassarian CK, Myers SA et al. Prostanoid receptors: subtypes and signaling. Annu Rev Pharmacol Toxicol 2001;41: 661–690.
21 Fujino H, Xu W, Regan J. Prostaglandin E2 induced functional expression of early growth response factor-1 by EP4, but not EP2, prostanoid receptors via the phosphatidylinositol 3-kinase and extracellular signal-regulated kinases. J Biol Chem 2003;278: 12151–12156.
22 Sugimoto Y, Narumiya S. Prostaglandin E receptors. J Biol Chem 2007;282:11613–11617.
23 FitzGerald GA. Coxibs and cardiovascular disease. N Engl J Med 2004;351:1709–1711.
24 Graham DJ. COX-2 inhibitors, other NSAIDs, and cardiovascular risk: The seduction of common sense. JAMA 2006;296: 1653–1666.
25 Guo Y, Tukaye DN, Wu WJ et al. The COX-2/PGI2 receptor axis plays an obligatory role in mediating the cardioprotection conferred by the late phase of ischemic preconditioning. PLoS One 2012;7:e41178. doi: 10.1371/journal.pone. 0041178.
26 Stylianou S, Clarke RB, Brennan K. Aberrant activation of notch signaling in human breast cancer. Cancer Res 2006;66:1517–1525.
27 Chen J, Imanaka N, Chen J et al. Hypoxia potentiates notch signaling in breast cancer leading to decreased E-cadherin expression and increased cell migration and invasion. Br J Cancer 2010;102:351–360. doi: 10.1038/sj.bjc.6605486.
28 Matsuda Y, Schlange T, Oakeley EJ et al. WNT signaling enhances breast cancer cell motility and blockade of the WNT pathway by sFRP1 suppresses MDA-MB-231 xenograft growth. Breast Cancer Res 2009;11:R32. doi: 10.1186/bcr2317.
29 Dey N, Barwick BG, Moreno CS et al. Wnt signaling in triple negative breast cancer is associated with metastasis. BMC Cancer 2013;13:537. doi: 10.1186/1471-2407-13-537.
30 Jang GB, Hong IS, Kim RJ et al. Wnt/β-catenin Small-molecule inhibitor CWP232228 preferentially inhibits the growth of breast cancer stem-like cells. Cancer Res 2015;75: 1691–1702. Apr 15; doi: 10.1158/0008-5472.CAN-14-2041. Epub 2015 Feb 6.
31 Buchanan FG, DuBois RN. Connecting COX-2 and Wnt in cancer. Cancer Cell 2006;9:6–8.
32 Howe LR, Chang SH, Tolle KC et al. HER2/neu induced mammary tumorigenesis and angiogenesis are reduced in cyclooxygenase-2knockout mice. Cancer Res 2005;65:10113–10119.
33 Howe LR, Subbaramaiah K, Patel J et al. Celecoxib, a selective cyclooxygenase 2 inhibitor, protects against human epidermal growth factor receptor 2 (HER-2)/neu-induced breast cancer. Cancer Res 2002;62: 5405–5407.
34 Bhattacharjee R, Timoshenko A, Cai J et al. Relationship between cyclooxygenase-2 and human epidermal growth factor receptor 2 in vascular endothelial growth factor C upregulation and lymphangiogenesis in human breast cancer. Cancer Sci 2010;101:2026–2032.
35 Majumder M, Tutunea-Fatan E, Xin X et al. Co-expression of α9β1 integrin and VEGF-D confers lymphatic metastatic ability to a human breast cancer cell line MDA-MB-468LN. PLoS One 2012;7:e35094. doi: 10.1371/journal. pone. 0035094.
36 Dontu G, Abdallah W, Foley J et al. In vitro propagation and transcriptional profiling of human mammary stem/progenitor cells. Genes Dev 2003;17:1253–1270.
37 Croker AK, Allan AL. Inhibition of aldehyde dehydrogenase (ALDH) activity reduces chemotherapy and radiation resistance of stem-like ALDHhiCD44+ human breast cancer cells. Breast Cancer Res Treat 2012;133: 75–87. doi: 10.1007/s10549-011-1692-y.
38 Hess DA, Craft TP, Wirthlin L et al. Widespread nonhematopoietic tissue distribution by transplanted human progenitor cells with high aldehyde dehydrogenase activity. Stem Cells 2008;26:611–620.
39 Quail DF, Zhang G, Walsh LA et al. Embryonic morphogen nodal promotes breast cancer growth and progression. PLoS One 2012;7:e48237. doi: 10.1371/journal. pone.0048237.
40 Jadeski LC, Lala PK. Nitric oxide synthase inhibition by N G-nitro-l-arginine methyl ester inhibits tumor-induced angiogenesis in mammary tumors. Am J Pathol 1999;155: 1381–1390.
41 http://cancergenome.nih.gov/.
42 Singh B, Cook KR, Vincent L et al. Role of COX-2 in tumorospheres derived from a breast cancer cell Line. J Surg Res 2011;168: e39–e49. doi: 10.1016/j.jss. 2010.03.003.
43 Kundu N, Ma X, Kochel T et al. Prostaglandin E receptor EP4 is a therapeutic target in breast cancer cells with stem-like properties. Breast Cancer Res Treat 2014;143:19–31.
44 Ma X, Holt D, Kundu N et al. A prostaglandin E (PGE) receptor EP4 antagonist protects natural killer cells from PGE2-mediated immunosuppression and inhibits breast cancer metastasis. Oncoimmunology 2013;12: e22647.
45 Pozzi A, Yan X, Macias-Perez I et al. Colon carcinoma cell growth is associated with prostaglandin E2/EP4 receptor-evoked ERK activation. J Biol Chem 2004;279:29797–29804.
46 George RJ, Sturmoski MA, Anant S et al. EP4 mediates PGE2 dependent cell survival through the PI3 kinase/AKT pathway. Prostaglandins Other Lipid Mediat 2007;83:112–120.
47 Kim JI, Lakshmikanthan V, Frilot N et al. Prostaglandin E2 promotes lung cancer cell migration via EP4-betaArrestin1-c-src signalsome. Mol Cancer Res 2010;8:569–577.
48 Yu X, Zou J, Ye Z et al. Notch signaling activation in human embryonic stem cells is required for embryonic, but not trophoblastic, lineage commitment. Cell Stem Cell 2008;2:461–471. doi: 10.1016/j.stem.2008.03.001.
49 Blauwkamp TA, Nigam S, Ardehali R et al. Endogenous Wnt signalling in human embryonic stem cells generates an equilibrium of distinct lineage-specified progenitors. Nat Commun 2012;3:1070. doi: 10.1038/ncomms2064.
50 Jang GB, Hong IS, Kim RJ et al. Wnt/β-catenin Small-molecule inhibitor CWP232228 preferentially inhibits the growth of breast cancer stem-like cells. Cancer Res 2015;75: 1691–1702. doi: 10.1158/0008-5472.CAN-14-2041.
51 Liou JY, Ellent DP, Lee S et al. Cyclooxygenase-2-derived prostaglandin E2 protects mouse embryonic stem cells from apoptosis. Stem Cells 2007;25:1096–1103.
52 Aguirre-Ghiso JA. Models, mechanisms and clinical evidence for cancer dormancy. Nat Rev Cancer 2007;7:834–846.


See www.StemCells.com for supporting information available online.

